



Contents lists available at ScienceDirect

Particuology

journal homepage: www.elsevier.com/locate/partic



Implementation and validation of a volume-of-fluid and discrete-element-method combined solver in OpenFOAM

Linmin Li^a, Baokuan Li^{b,*}

^a College of Energy and Electrical Engineering, Hohai University, Nanjing 211100, China

^b Department of Thermal Engineering, Northeastern University, Shenyang 110819, China

ARTICLE INFO

Article history:

Received 7 March 2017

Received in revised form 4 September 2017

Accepted 8 September 2017

Available online xxx

Keywords:

Gas–liquid–solid flow

Volume of fluid

Discrete element method

OpenFOAM

ABSTRACT

Numerous gas–liquid–solid flows exist in chemical engineering and metallurgical processes. Numerical modeling is an important topic that can be used to improve the design and investigate the operating conditions of these processes. The complicated interphase interaction within such three-phase systems, which include free surfaces and discrete phases, poses challenges in the existing methods. We implemented a volume-of-fluid (VOF) and discrete-element-method (DEM) combined solver, which should be useful for modeling the gas–liquid–solid systems, within the OpenFOAM framework. The Du Plessis and Masliyah drag force, added mass force, and capillary force were considered for fluid–particle coupling. The VOF–DEM solver was tested in three different cases, namely, particles in pure gas, particle collision in water, and gas–liquid–solid three-phase dam break. The results were validated against previous experiments and good agreement was obtained between the simulations and the experiments, which indicates the accuracy and suitability of this VOF–DEM solver for gas–liquid–solid systems.

© 2017 Chinese Society of Particuology and Institute of Process Engineering, Chinese Academy of Sciences. Published by Elsevier B.V. All rights reserved.

Introduction

Numerous gas–liquid–solid flows exist in industrial operations, such as in wet ball milling, ladle metallurgy and other chemical processes. For several decades, numerical models have gained considerable attention to investigate fluid–particle flows, especially in gas–solid systems, e.g., in fluidized beds and pneumatic conveying. Significant progress has been made to model systems with single fluid and solid particles (Alobaid & Eppler, 2013; Cundall & Strack, 1979; Deen, Annaland, van der Hoef, & Kuipers, 2007; Huang, 2011; Luo, Wang, Yang, Hu, & Fan, 2017; Tsuji, Tanaka, & Ishida, 1992; Wang, Lu, Zhang, Shi, & Li, 2010; Xu & Yu, 1997), especially for gas–solid systems. Among the simulation approaches for such systems, the two-fluid model (TFM) (Anderson & Jackson, 1967) and the discrete element method (DEM) (Cundall & Strack, 1979; Tsuji et al., 1992) are the two most well-known methods. These approaches have been implemented in OpenFOAM (The OpenFOAM Foundation, 2014a, 2014b), which can refer to the solvers of TwoPhaseEulerFoam and DPMFoam. Thus far, except for the multi-fluid solver, there is no suitable solver with the particle

behavior fully resolved for gas–liquid–solid three-phase systems in OpenFOAM.

An easy way to treat phases in gas–liquid–solid three-phase systems is in a uniform Eulerian coordinate, which is less computationally demanding, and so, it is useful in large-scale systems (Li & Zhong, 2015; Panneerselvam, Savithri, & Surender, 2009). The volume of fluid (VOF) and DEM combined method, which is considered an effective solution for gas–liquid–solid systems, was proposed by Li, Zhang, and Fan (1999) and Zhang, Li, and Fan (2000a, 2000b) in two dimensions. Chen and Fan (2004) and Van Sint Annaland, Deen, and Kuipers (2005) extended this approach to three dimensions by combining a front-tracking method and the DEM. Recently, other interface tracking approaches have been carried out combined with the DEM. Washino, Tan, Hounslow, and Salman (2013) presented a coupling of the DEM and a constrained interpolation profile to simulate the nucleation process in wet granulation. Sun et al. (Sun, Sakai, Sakai, & Yamada, 2014; Sun & Sakai, 2015) proposed two approaches by combining the moving particle semi-implicit (MPS) or VOF method with the DEM to simulate liquid–solid flows that involve free surfaces. The MPS (Koshizuka & Oka, 1996) can be used to deal with free surfaces based on Lagrangian particle methods that are similar to the smoothed particle hydrodynamics (SPH) (Monaghan, 1988). Within the context of Lagrangian methods, although the advection, deformation and topological change of the fluid interface can be simplified, one drawback is the need

* Corresponding author.

E-mail address: libk@smm.neu.edu.cn (B. Li).

for large numbers of particles to produce simulations of equivalent resolution.

The motivation for this work is the implementation of a VOF–DEM combined solver in OpenFOAM, which is the most popular open-source computational fluid dynamics (CFD) code in academia and in industry. OpenFOAM version 3.0.0 was used and the developed solver is termed interDPMFoam. The fluid interface was solved by using the VOF method with considering the particle volume fraction, whereas the particle trajectory was calculated by using Newton's second law. The particle–particle or particle–wall interactions were resolved directly by using the DEM. For fluid–particle coupling, the [Du Plessis and Masliyah \(1991\)](#) drag relationship, which was proposed originally for total porosities in fluid–solid systems, was used. To consider the capillary force that was induced by the gas–liquid interface, an additional interfacial force was incorporated into the solver. Different cases were studied and the results were compared with experiments to test the new solver, and to determine its adequacy and suitability for simulations of gas–liquid–solid three-phase flows.

Model description

Volume-of-fluid method

The interface-tracking algorithm is based on the VOF method by solving a single set of momentum equations and by tracking the volume fraction of the liquid phase. OpenFOAM uses an improved version of the compressive interface-capturing scheme for arbitrary meshes (CICSAM) from Ubbink's work ([Ubbink, 1997](#)), in which a supplementary interface-compression velocity \mathbf{u}_c is defined in the vicinity of the interface to steepen the gradient of the volume fraction and to improve the interface resolution. The conservation equation for the liquid volume fraction (γ) is solved in the following form:

$$\frac{\partial \gamma}{\partial t} + \nabla \cdot (\gamma \mathbf{u}) + \nabla \cdot (\mathbf{u}_c \gamma (1 - \gamma)) = 0, \quad (1)$$

where the compression velocity is calculated as ([Weller, 2008](#)):

$$\mathbf{u}_c = \min(C_\gamma |\mathbf{u}|, \max(|\mathbf{u}|)) \frac{\nabla \gamma}{|\nabla \gamma|}, \quad (2)$$

where C_γ is a constant that is used to control the intensity of compression. The momentum equation for the gas–liquid mixture is solved in the following form:

$$\rho \left(\frac{\partial (\varepsilon \mathbf{u})}{\partial t} + \nabla \cdot (\varepsilon \mathbf{u} \mathbf{u}) \right) = \varepsilon (-\nabla P + \nabla \cdot (\mu (\nabla \mathbf{u} + \nabla \mathbf{u}^T))) + \rho \mathbf{g} + \mathbf{F}_s + \mathbf{F}_p, \quad (3)$$

where ρ and μ are the density and viscosity of the mixture that are defined as:

$$\rho = \gamma \rho_l + (1 - \gamma) \rho_g, \quad (4)$$

$$\mu = \gamma \mu_l + (1 - \gamma) \mu_g, \quad (5)$$

ε is the void fraction in an Eulerian cell, which is calculated as:

$$\varepsilon = \max \left(1 - \frac{1}{V_{\text{cell}}} \sum_{p \in \text{cell}} f_p V_p, \varepsilon_{\min} \right), \quad (6)$$

where V_{cell} and V_p are the cell and particle volume, respectively, and f_p is the fractional volume of a particle that resides in a cell under consideration. ε_{\min} is a value that is set to be slightly larger than 0 to avoid the cell from being occupied fully by a particle.

The surface tension is evaluated per unit volume by using the continuum-surface-force model ([Brackbill, Kothe, & Zemach, 1992](#)):

$$\mathbf{F}_s = \sigma \kappa \nabla \gamma, \quad (7)$$

where σ is the surface-tension coefficient and the curvature κ of the free surface is calculated as:

$$\kappa = -\nabla \cdot (\nabla \gamma / |\nabla \gamma|). \quad (8)$$

Discrete-element model

The translational and rotational motions of each individual particle with mass m_p are calculated from Newton's second law:

$$m_p \frac{d\mathbf{u}_p}{dt} = m_p \mathbf{g} \left(1 - \frac{\rho}{\rho_p} \right) + \mathbf{F}_c + \mathbf{F}_p, \quad (9)$$

$$I_p \frac{d\boldsymbol{\omega}_p}{dt} = \mathbf{T}_p, \quad (10)$$

where I_p is the moment of inertia, which is equal to $2m_p R_p^2/5$; $\boldsymbol{\omega}_p$ is the rotational velocity, and \mathbf{T}_p represents the torque that is caused by the contact force. The particle–particle or particle–wall contact force \mathbf{F}_c is determined from their overlap during a finite collision time and is calculated according to the model as proposed by [Cundall and Strack \(1979\)](#), which consists of a spring, a dash-pot and a slider, and the Hertzian spring-dashpot model is used. Details on the contact force and the determination of parameters can be found in [Tsuji et al. \(1992\)](#) and [Li, Li, and Liu \(2017\)](#).

Fluid–particle coupling

A two-way coupling is achieved via the sink term \mathbf{F}_p , which represents the momentum exchange between fluid and particles, such as drag force, virtual mass force, and Basset force. The drag force is written as:

$$\mathbf{F}_d = \frac{V_p \beta}{1 - \varepsilon} (\mathbf{u} - \mathbf{u}_p), \quad (11)$$

where β represents the interphase momentum transfer coefficient from drag. Several drag relationships exist and details can be found in [Li et al. \(2017\)](#). In this work, a continuous relationship with the change in porosity as proposed by [Du Plessis and Masliyah \(1991\)](#), which is suitable for gas and liquid is used:

$$\beta = A \frac{(1 - \varepsilon)^2}{\varepsilon} \frac{\mu}{d_p^2} + B (1 - \varepsilon) \frac{\rho}{d_p} |\mathbf{u} - \mathbf{u}_p|, \quad (12)$$

where the coefficients A and B are given as:

$$A = \frac{26.8 \varepsilon^3}{(1 - \varepsilon)^{2/3} \left(1 - (1 - \varepsilon)^{1/3} \right) \left(1 - (1 - \varepsilon)^{2/3} \right)^2}, \quad (13)$$

$$B = \frac{\varepsilon^2}{\left(1 - (1 - \varepsilon)^{2/3} \right)^2}. \quad (14)$$

As indicated by several researchers ([Huang, 2011](#); [Li et al., 1999](#); [Zhang et al., 2000a, 2000b](#)), the added mass force has an important effect on particles in liquid. In this work, we consider the added mass force for fluid–particle coupling, which is written as:

$$\mathbf{F}_{am} = 0.5 V_p \rho \frac{d(\mathbf{u} - \mathbf{u}_p)}{dt}. \quad (15)$$

An additional force F_i , which corresponds with the capillary force that is induced by the gas–liquid interface is defined as (Sun & Sakai, 2015):

$$F_i = C m_p \nabla \gamma, \quad (16)$$

where C is a coefficient that can be defined when the effect of surface tension that is caused by the gas–liquid interface is considered, but this is a complicated issue. Because this work does not consider the condition where the capillary force is important, the determination of coefficient is not discussed. Finally, fluid–particle coupling is achieved by the volume averaging of particle forces in an Eulerian cell.

Case studies

Particles in pure gas

The model is adopted to cases of gas–solid flows in a dense bed with gas injection. Two cases of (1) single-bubble flow and (2) spout–fluidization were studied. The first one was set up according to the experiment by Bokkers (2005), who studied the evolution of bubble size and shape in a fluidized bed where a single bubble was injected from a central jet. The background velocity was maintained via a porous plate distributor and the bubble was injected through an inlet pulse for a short duration. The second case was carried out according to the work by Link, Cuypers, Deen, and Kuipers (2005) where a spouted fluidized bed was set up and different flow regimes were specified. Of the flow regimes, spout–fluidization involves a periodic fluctuating pressure drop, and can be used easily for numerical model testing. Thus, the spout–fluidization regime has been chosen in this test. The simulation parameters for the current case include the material properties, the geometric parameters, and the boundary conditions are listed in Table 1. For all the cases, uniform meshes were used and the grid size was 5 mm.

For single-bubble flow, the simulation results as compared with the experimental observations are shown in Fig. 1. Instantaneous states during bubble growth and propagation are displayed. The model captures the interaction of particles with the jet: the bubble grows from 0 to 0.3 s and then collapses, particles in front of the jet rise, whereas those in the wake of the bubble are dragged into

Table 1
Parameters for simulation.

Parameters	Values	
Young's Modulus (Pa)	6×10^{10}	
Poisson's ratio	0.23	
Coefficient of restitution	0.97	
Coefficient of friction	0.09	
Density (kg/m^3)	2526 (glass), 1.2 (air)	
Viscosity of air (Pa s)	1.85×10^{-5}	
Particle diameter (mm)	2.5	
Gravitational acceleration (m/s^2)	9.81	
Parameters	Single-bubble flow	Spout–fluidization
Domain size (m)	$0.3 \times 0.015 \times 0.6$	$0.15 \times 0.015 \times 0.75$
Number of particles	52,000	24,500
Inlet size (m)	0.015×0.015	0.01×0.015
Background velocity (m/s)	1.25	1.5
Jet velocity (m/s)	20	30
Pulse duration (s)	0.15	–
Time step (s)	1×10^{-5}	1×10^{-5}

the bubble center. The predicted flow behaviors coincide with the experiment and a reasonable agreement is obtained.

For spout–fluidization, a snapshot during the simulation is shown in Fig. 2(a) and is compared with the experimental image (Link et al., 2005) (Fig. 2(b)). The simulated spouting characteristics and the bed height under this condition agree well with the experimental results. In this regime, particles in the upper part of the bed are fluidized and move gently. The spout channel is blocked periodically by particles that move into the spout channel from the annulus, and the pressure drop fluctuates regularly. For a more detailed and clearer observation, an animation of the transient gas–solid flow with the evolution of a time-averaged vertical gas velocity is provided as a supplementary material. For a quantitative comparison, the time-averaged vertical gas velocity and particle flux were compared with the results from Link et al. (2005), as shown in the curves in Fig. 2(c). The comparison agrees well. Thus, the solver is suitable for predicting interactions between gas and particles.

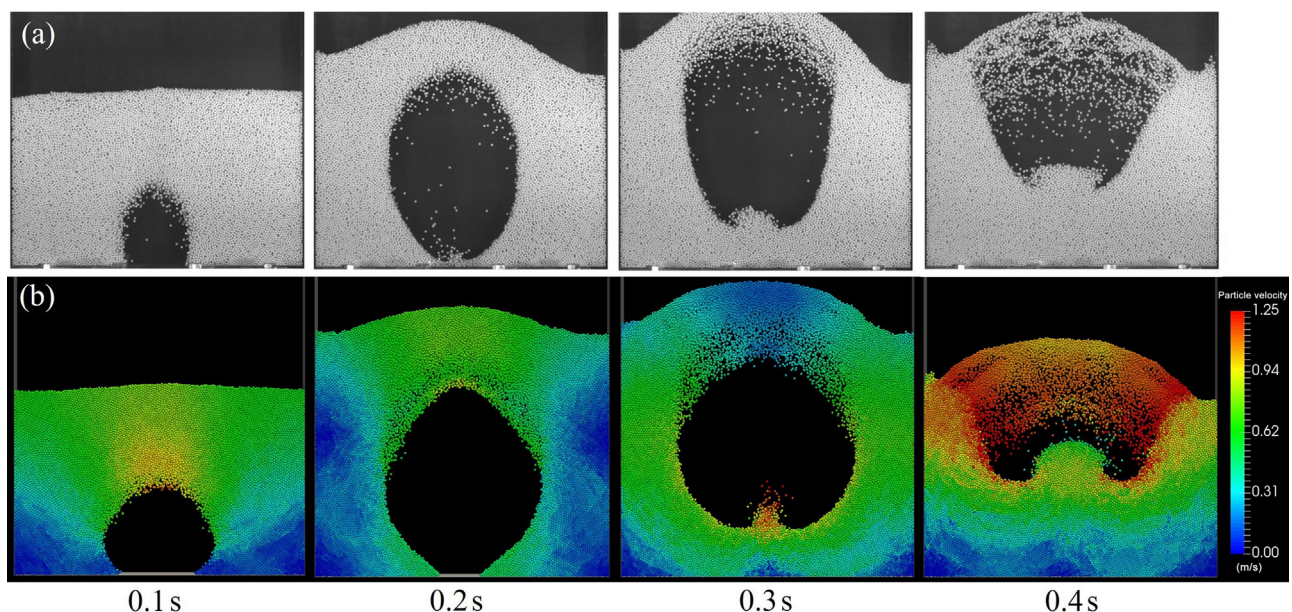


Fig. 1. Comparison between (a) experiment (Bokkers, 2005) and (b) simulation for single-bubble flow.

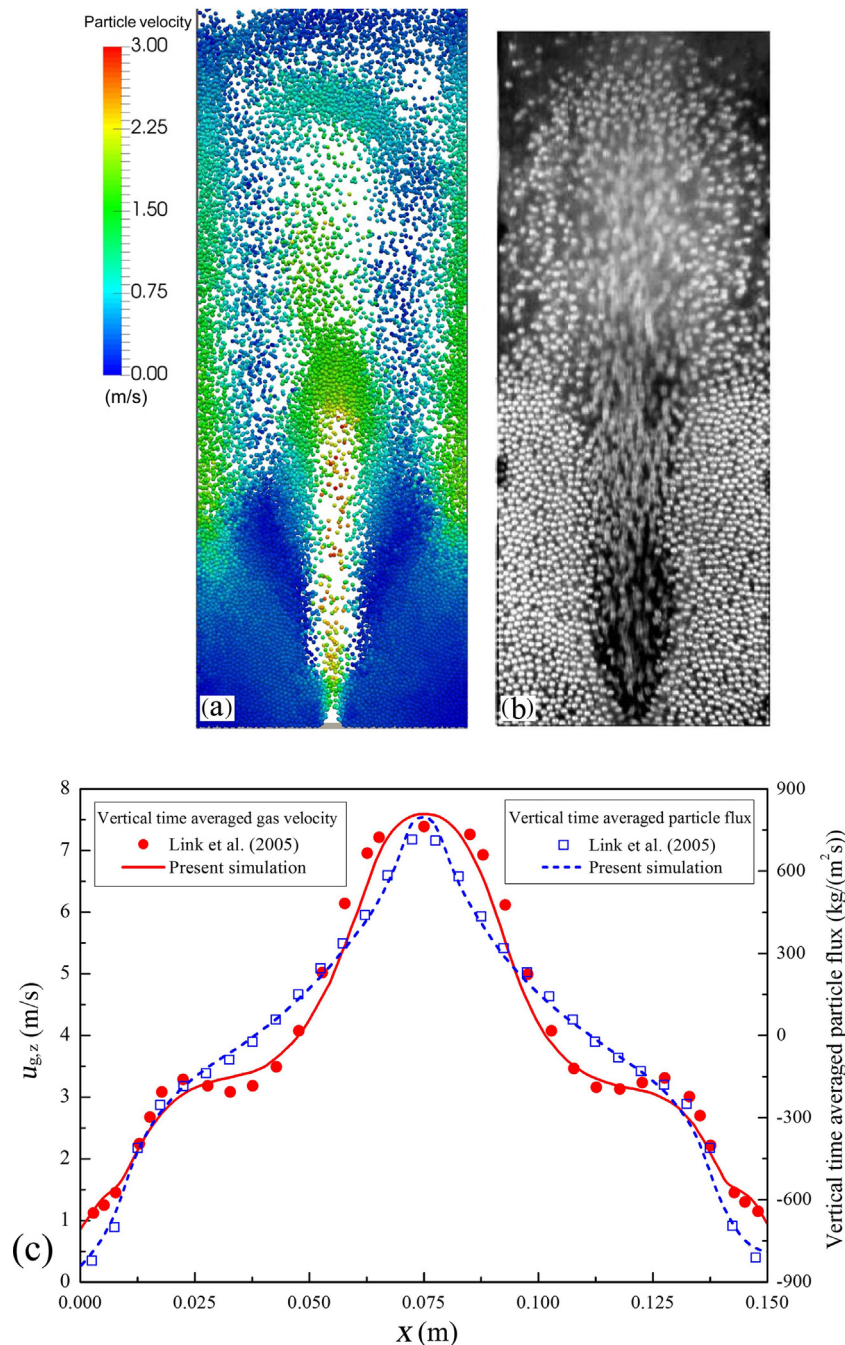


Fig. 2. Comparison between (a) simulation and (b) experiment (Link et al., 2005) for spout fluidization, and (c) comparison of time-averaged vertical gas velocity and particle flux between the results of Link et al. (2005) and this simulation.

Particle collision in water

To investigate the liquid–solid interaction when using the adopted VOF–DEM model, the model is adapted to a process of collision between two particles in the liquid phase. The experiment was carried out by Zhang, Fan, Zhu, Pfeffer, and Qi (1999) where an oblique collision of two 2-mm-diameter glass beads was studied. The material properties, such as Young's Modulus of the particles, is shown in Table 1. Water is used as the liquid phase. The approaching particle is released from four particle diameters above the particle that rests at the base of the vessel. Particle motion was recorded by a high-speed camera and the trajectories of the particle centers were measured from the recorded frames. The initial state of this simulation is set as shown in Fig. 3(a): two particles with

centroid positions of ($x = 5$ mm, $z = 1$ mm) and ($x = 4$ mm, $z = 9$ mm) were placed on the plane $y = 0.05$ m in a 0.1 m \times 0.1 m \times 0.1 m box. The box was filled partially with water to a height of 0.085 m. The trajectories of the two particles that were recorded in previous experiments and simulations (Zhang et al. 1999) are compared with this simulation in Fig. 3(b). The trajectories show that a reasonable agreement is obtained, although this VOF–DEM model predicts a slightly further rebound point.

Gas–liquid–solid dam break

The VOF–DEM solver was used in a case that included interactions among three phases of gas, liquid, and solid. The case was set up according to the experiment that was carried out by Sun

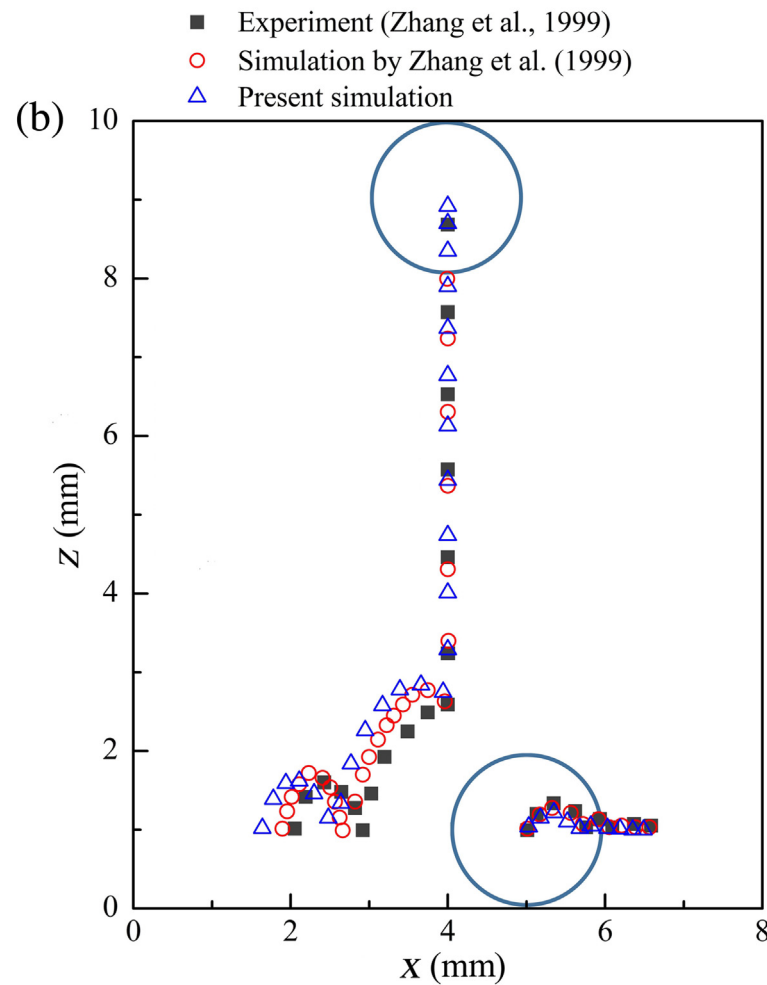
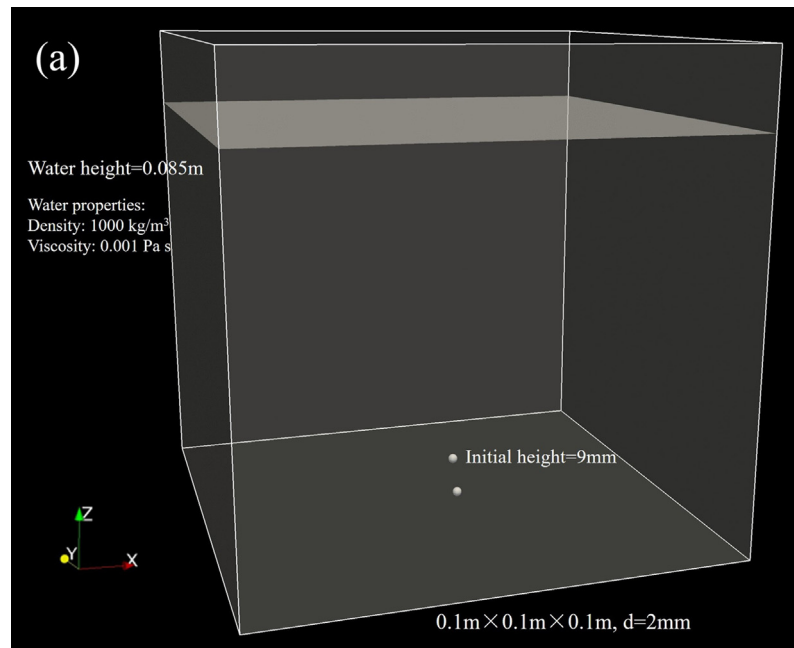


Fig. 3. (a) Initial state and parameters for particle collision in water and (b) comparison of experimental (Zhang et al., 1999) and simulated (Zhang et al., 1999 and this study) trajectories during oblique collision of two particles in water.

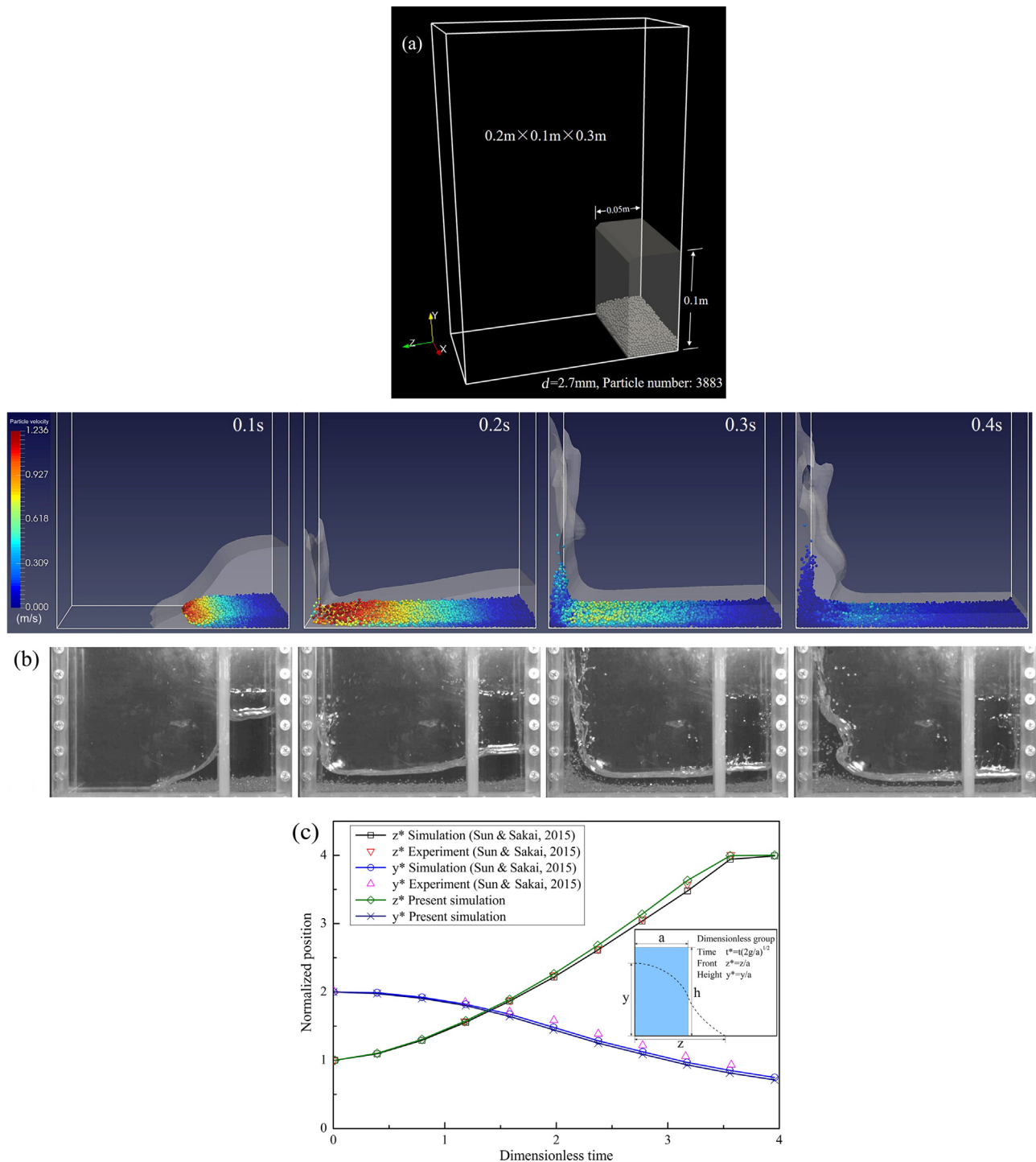


Fig. 4. (a) Initial state and parameters for gas–liquid–solid three-phase dam break, (b) experimental (Sun & Sakai, 2015) and simulated gas–liquid interface evolution and particle motion during dam-break flow, with dot colors representing particle move speeds, and (c) experimental (Sun & Sakai, 2015) and simulated (Sun & Sakai, 2015, and this study) normalized water front position and water height evolutions.

and Sakai (2015), for which the initial state is shown in Fig. 4(a). The length, width, and height of the computational domain were 0.2, 0.1, and 0.3 m, respectively. A non-slip boundary condition was established at all the walls, whereas the top was set as a pressure outlet. The reservoir with a length of 0.05 m holds a solid bed of glass beads and a box of water with a height of 0.1 m. The number of 2.7-mm-diameter glass beads was 3883. The initial state was obtained by performing a simulation of random packing until the particles had settled.

Fig. 4(b) shows snapshots of the gas–liquid–solid three-phase dam-break flow from $t = 0.1$ to 0.4 s with an interval of 0.1 s. During dam breaking, the mixture column flows to the other side to form an elongating surge front. The particles were dragged by liquid and the motion was captured as rendered by scattered dots that were colored according to their velocities. Particles reached the left wall at ~ 0.2 s and were shoved up. After 0.4 s, subject to the impact of water falling down, particles were dragged down again. A comparison of the simulation results with the experimen-

tal data (Sun & Sakai, 2015) shows that the air–water interface evolution and the particle motion agree well with the captured images. Details on the three-phase dam-break simulation are visible in the video in the supplementary materials. The evolution of a dimensionless front and a water height with dimensionless time as illustrated in Fig. 4(c) is compared with the results as provided by Sun and Sakai (2015). Agreement is obtained quantitatively, which indicates the accuracy and suitability of the VOF–DEM solver for the gas–liquid–solid systems. Some differences exist between this model and that of Sun and Sakai (2015), such as the treatment of boundaries, the particle–collision model and fluid–particle interactions. Fluid–particle interactions may affect the flow behavior significantly. As seen in the tests, the forces for fluid–particle coupling as used in this work were also suitable. Additionally, an interfacial force was used to consider the capillary force, but its accuracy and applicability were not discussed. Those who work with problems where capillary force is important should choose the coefficient of capillary force carefully.

Conclusions

A VOF–DEM solver was implemented within the OpenFOAM framework to simulate gas–liquid–solid flows, including the interface and discrete particles. The solver was tested by simulating three cases, namely, particles in pure gas, particle collision in water, and gas–liquid–solid three-phase dam break. The results were compared with experiments that were carried out by Bokkers (2005), Link et al. (2005), Zhang et al. (1999), and Sun and Sakai (2015) and qualitative agreement was obtained. The solver is suitable for systems that contain discrete particles and two continuous phases with a distinct interface. It is also suitable for flows with particles in a pure fluid. Because the gas–liquid–solid flows that were studied are quite simple, more detailed work should be conducted. Particle behavior near the interface from a microscopic perspective is not discussed in this work.

Acknowledgement

This work was supported by the National Natural Science Foundation of China, Grant No. 51210007.

Appendix A. Supplementary data

Supplementary data associated with this article can be found, in the online version, at <https://doi.org/10.1016/j.partic.2017.09.007>.

References

- Alobaid, F., & Epple, B. (2013). Improvement, validation and application of CFD/DEM model to dense gas–solid flow in a fluidized bed. *Particuology*, 11(5), 514–526.
- Anderson, T. B., & Jackson, R. (1967). Fluid mechanical description of fluidized beds. *Equations of motion. Industrial & Engineering Chemistry Fundamentals*, 6(4), 527–539.
- Bokkers, G. A. (2005). *Multi-level modelling of the hydrodynamics in gas phase polymerisation reactors (Doctoral dissertation)*. The Netherlands: University of Twente.

- Brackbill, J. U., Kothe, D. B., & Zemach, C. (1992). A continuum method for modeling surface tension. *Journal of Computational Physics*, 100(2), 335–354.
- Chen, C., & Fan, L. S. (2004). Discrete simulation of gas–liquid bubble columns and gas–liquid–solid fluidized beds. *AIChE Journal*, 50(2), 288–301.
- Cundall, P. A., & Strack, O. D. (1979). A discrete numerical model for granular assemblies. *Geotechnique*, 29(1), 47–65.
- Deen, N. G., Annaland, M. V. S., Van der Hoef, M. A., & Kuipers, J. A. M. (2007). Review of discrete particle modeling of fluidized beds. *Chemical Engineering Science*, 62(1–2), 28–44.
- Du Plessis, J. P., & Masliyah, J. H. (1991). Flow through isotropic granular porous media. *Transport in Porous Media*, 6(3), 207–221.
- Huang, X. (2011). CFD modeling of liquid–solid fluidization: Effect of drag correlation and added mass force. *Particuology*, 9(4), 441–445.
- Koshizuka, S., & Oka, Y. (1996). Moving-particle semi-implicit method for fragmentation of incompressible fluid. *Nuclear Science and Engineering*, 123(3), 421–434.
- Li, L., Li, B., & Liu, Z. (2017). Modeling of spout-fluidized beds and investigation of drag closures using OpenFOAM. *Powder Technology*, 305, 364–376.
- Li, W., & Zhong, W. (2015). CFD simulation of hydrodynamics of gas–liquid–solid three-phase bubble column. *Powder Technology*, 286, 766–788.
- Li, Y., Zhang, J., & Fan, L. S. (1999). Numerical simulation of gas–liquid–solid fluidization systems using a combined CFD–VOF–DPM method: Bubble wake behavior. *Chemical Engineering Science*, 54(21), 5101–5107.
- Link, J. M., Cuypers, L. A., Deen, N. G., & Kuipers, J. A. M. (2005). Flow regimes in a spout–fluid bed: A combined experimental and simulation study. *Chemical Engineering Science*, 60(13), 3425–3442.
- Luo, K., Wang, S., Yang, S., Hu, C., & Fan, J. (2017). Computational fluid dynamics–discrete element method investigation of pressure signals and solid back-mixing in a full-loop circulating fluidized bed. *Industrial & Engineering Chemistry Research*, 56(3), 799–813.
- Monaghan, J. J. (1988). An introduction to SPH. *Computer Physics Communications*, 48(1), 89–96.
- Panneerselvam, R., Savithri, S., & Surender, G. D. (2009). CFD simulation of hydrodynamics of gas–liquid–solid fluidised bed reactor. *Chemical Engineering Science*, 64(6), 1119–1135.
- Sun, X., & Sakai, M. (2015). Three-dimensional simulation of gas–solid–liquid flows using the DEM–VOF method. *Chemical Engineering Science*, 134, 531–548.
- Sun, X., Sakai, M., Sakai, M. T., & Yamada, Y. (2014). A Lagrangian–Lagrangian coupled method for three-dimensional solid–liquid flows involving free surfaces in a rotating cylindrical tank. *Chemical Engineering Journal*, 246, 122–141.
- The OpenFOAM Foundation. (2014a). *Discrete particle modelling*. Retrieved from <http://openfoam.org/release/2-3-0/dpm>.
- The OpenFOAM Foundation. (2014b). *Multiphase modelling*. Retrieved from <http://openfoam.org/release/2-3-0/multiphase/#phase-interaction>.
- Tsuji, Y., Tanaka, T., & Ishida, T. (1992). Lagrangian numerical simulation of plug flow of cohesionless particles in a horizontal pipe. *Powder Technology*, 71(3), 239–250.
- Ubbink, O. (1997). *Numerical prediction of two fluid systems with sharp interfaces (Doctoral dissertation)*. UK: Imperial College, University of London.
- van Sint Annaland, M., Deen, N. G., & Kuipers, J. A. M. (2005). Numerical simulation of gas–liquid–solid flows using a combined front tracking and discrete particle method. *Chemical Engineering Science*, 60(22), 6188–6198.
- Wang, W., Lu, B., Zhang, N., Shi, Z., & Li, J. (2010). A review of multiscale CFD for gas–solid CFB modeling. *International Journal of Multiphase Flow*, 36(2), 109–118.
- Washino, K., Tan, H. S., Hounslow, M. J., & Salman, A. D. (2013). Meso-scale coupling model of DEM and CIP for nucleation processes in wet granulation. *Chemical Engineering Science*, 86, 25–37.
- Weller, H. G. (2008). *A new approach to VOF-based interface capturing methods for incompressible and compressible flow*. Technical Report TR/HGW/04, OpenCFD Ltd.
- Xu, B. H., & Yu, A. B. (1997). Numerical simulation of the gas–solid flow in a fluidized bed by combining discrete particle method with computational fluid dynamics. *Chemical Engineering Science*, 52(16), 2785–2809.
- Zhang, J., Fan, L. S., Zhu, C., Pfeffer, R., & Qi, D. (1999). Dynamic behavior of collision of elastic spheres in viscous fluids. *Powder Technology*, 106(1), 98–109.
- Zhang, J., Li, Y., & Fan, L. S. (2000a). Discrete phase simulation of gas–liquid–solid fluidization systems: Single bubble rising behavior. *Powder Technology*, 113(3), 310–326.
- Zhang, J., Li, Y., & Fan, L. S. (2000b). Numerical studies of bubble and particle dynamics in a three-phase fluidized bed at elevated pressures. *Powder Technology*, 112(1), 46–56.